Propagation of coherent and partially coherent pulses through one-dimensional photonic crystals

Wang Li-gang,[1,2] Liu Nian-hua,[1,3] Lin Qiang,[1,2] and Zhu Shi-yao[1,2]
[1]*Department of Physics, Hong Kong Baptist University, Kowloon Tong, Hong Kong, China*
[2]*Department of Physics, Zhejiang University, Hangzhou, 310027, China*
[3]*Department of Physics, Nanchang University, Nanchang 330047, China*
(Received 18 November 2003; revised manuscript received 20 February 2004; published 2 July 2004)

The propagation of coherent and partially coherent light pulses through a one-dimensional photonic crystal (1DPC) is investigated. The dependence of the evolution of the pulses inside the 1DPC on incident angles and the effect of the coherence of the pulses on the propagation properties are discussed. The evolution of a pulse inside the 1DPC is affected by the coherence of the pulse. As the coherence decreases, superluminal propropgation changes to subluminal propagation.

DOI: 10.1103/PhysRevE.70.016601 PACS number(s): 42.25.Bs, 42.70.Qs, 42.50.Ar

I. INTRODUCTION

Photonic crystals have been intensively investigated in many studies [1,2]. The most essential property of the photonic crystals is the photonic band-gap structures (PBG's). Due to the analogy between light through a one-dimensional photonic crystal (1DPC) and an electron passing a tunneling barrier, the 1DPC is used as an optical barrier to investigate the tunneling time [3,4]. The experiments have shown that the tunneling time of a single photon (or a short pulse) through the 1DPC is superluminal [5–7]. One of the theoretical methods to study the dynamical behavior of a pulse through the 1DPC is the transfer matrix method [8].

Superluminal phenomena usually refer to the fact that the group velocity of a light pulse **[**given by $v_g = c(n(\omega) + \omega\{[dn(\omega)]/d\omega\})^{-1}$**]** in an anomalously dispersive medium can be larger than the light speed c in vacuum or even become negative [9–11]. Since the confirmation from the first experiment by Chu and Wong [12] in a number of experiments [5–7,13,14], the superluminal group velocity has been observed (for some good reviews, e.g., see Refs. [15,16]). All these results of the experimental and theoretical investigations are no violation of Einstein's causality. Recently, the mechanism of superluminal propagation has become a topic of hot debate [17]. Japha and Kurizki [18] emphasized that the interference between different causal paths plays a key role in the tunneling process. We have also shown that the coherence of a light pulse plays an important role for superluminal propagation in dispersive media from the theory of coherence for nonstationary light sources [19,20]. The superluminality of a light pulse passing through an anomalous dispersive medium will disappear when the coherence of light decreases.

In practice, any real light source is not fully coherent. In previous investigations, the pulse was assumed fully coherent and decomposed into an integral of all Fourier components. In the present paper, we will discuss the propagating properties of partially coherent pulses (PCP's) passing through a 1DPC under different incident angles. We find that the time delay between the coherent pulses and the partially coherent pulses through the 1DPC is different. This may be helpful to explain the discrepancy of the group delay time between experimental measurements and theoretical predictions. Furthermore, we extend our results to the cases of partially coherent light pulses passing through the 1DPC and discuss how the coherence of light affects the propagation dynamics of light pulses inside the 1DPC.

II. TRANSFER MAXTRIX FORMALISM FOR COHERENT PULSES

We consider the propagation of coherent light pulses passing through the 1DPC's. Our method involves solving the wave equation and then combining with the boundary condition, and finally obtaining the evolution solutions of light pulses inside the 1DPC's. It should be pointed out that our general results can be used under any incident angle for both the cases of TM and TE plane waves.

A. TM waves

Consider that the incident pulses are composed of TM plane waves as shown in Fig. 1. As is well known, in an

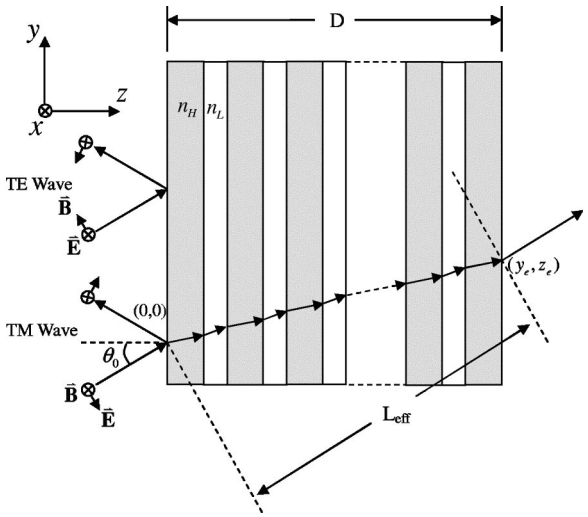

FIG. 1. Schematical diagram of the 1DPC [composed of the structure of $(HL)^N H$] under any incident angle for TM and TE waves.

inhomogeneous dielectric medium, Maxwell's equations lead to the following wave equation for the magnetic induced field $\vec{B}$ [21]:

$$\nabla^2\vec{B}(x,y,z,\omega)+\frac{\nabla\epsilon(x,y,z,\omega)}{\epsilon(x,y,z,\omega)}\times[\nabla\times\vec{B}(x,y,z,\omega)]+\frac{\omega^2}{c^2}\epsilon(x,y,z,\omega)\vec{B}(x,y,z,\omega)=0, \quad (1)$$

where $\epsilon(x,y,z,\omega)$ is the dielectric function of the medium and c is the speed of light in vacuum. Assume that the medium is homogeneous in each layer, so that we have $\nabla\epsilon(x,y,z,\omega)=0$ in each layer. We also assume that the magnetic-induced field is in the x direction as shown in Fig. 1 [i.e., $\vec{B}\equiv(B_x,0,0)$]. Therefore Eq. (1) can be written in a scalar form

$$\frac{d^2B_x(y,z,\omega)}{dy^2}+\frac{d^2B_x(y,z,\omega)}{dz^2}+\frac{\omega^2}{c^2}\epsilon(\omega)B_x(y,z,\omega)=0. \quad (2)$$

Here we use the method of Ref. [8] by solving Eq. (2) in each single layer and then integrating all Fourier components to obtain the temporal-spatial behavior of the pulse. For coherent pulses, the integral is a coherent superposition of all Fourier components including the forward waves and bakward waves with the complicated phase shifts.

For any incident angle, the general solution of Eq. (2) in the jth layer can be expressed as

$$B_x^{(j)}(y,z,\omega)=\exp[ik_y^{(j)}\Delta y^{(j)}]\{B_x^{(+)}(y_{j-1},z_{j-1},\omega)\exp[ik_z^{(j)}\Delta z^{(j)}]+B_x^{(-)}(y_{j-1},z_{j-1},\omega)\exp[-ik_z^{(j)}\Delta z^{(j)}]\}, \quad (3)$$

where $k_y^{(j)}=k_j\sin\theta_j$ and $k_z^{(j)}=k_j\cos\theta_j$, and k_j and θ_j are the wave number and refraction angle in the jth layer, respectively; $\Delta y^{(j)}=y-y_{j-1}$ and $\Delta z^{(j)}=z-z_{j-1}$ are the propagating distances in the y and z directions in the jth layer, respectively. The superscripts "+" and "−", respectively, denote the forward and backward waves. In this paper we simply assume the medium is nonmagnetic and stationary. From Maxwell's equations, we have the relation $\vec{E}(y,z,\omega)=[i/\omega n_j^2(\omega)]\nabla\times\vec{B}$ where $n_j(\omega)=\sqrt{\epsilon_j(\omega)}$ is the refraction index. Therefore we obtain the components of the electric field,

$$E_x^{(j)}(y,z,\omega)=0, \quad (4a)$$

$$E_y^{(j)}(y,z,\omega)=-\frac{\cos\theta_j}{cn_j(\omega)}\exp[ik_y^{(j)}\Delta y^{(j)}]\times\{B_x^{(+)}(y_{j-1},z_{j-1},\omega)\exp[ik_z^{(j)}\Delta z^{(j)}]-B_x^{(-)}(y_{j-1},z_{j-1},\omega)\exp[-ik_z^{(j)}\Delta z^{(j)}]\}, \quad (4b)$$

$$E_y^{(j)}(y,z,\omega)=-\frac{\sin\theta_j}{cn_j(\omega)}\exp[ik_y^{(j)}\Delta y^{(j)}]\times\{B_x^{(+)}(y_{j-1},z_{j-1},\omega)\exp[ik_z^{(j)}\Delta z^{(j)}]+B_x^{(-)}(y_{j-1},z_{j-1},\omega)\exp[-ik_z^{(j)}\Delta z^{(j)}]\}, \quad (4c)$$

which are polarized in the y-z plane. For the simplicity, we define

$$\psi_{1j}(y,z,\omega)=B_x^{(j)}(y,z,\omega), \quad (5a)$$

$$\psi_{2j}(y,z,\omega)=-cE_y^{(j)}(y,z,\omega), \quad (5b)$$

$$\psi_{3j}(y,z,\omega)=cE_z^{(j)}(y,z,\omega), \quad (5c)$$

such that the magnetic component $\psi_{1j}(y,z,\omega)$ and the "two electric components" $\psi_{2j}(y,z,\omega)$ and $\psi_{3j}(y,z,\omega)$ have the same unit. The electromagnetic fields in the x-y plane can be expressed by a two-component wave vector composed of $\psi_{1j}(y,z,\omega)$ and $\psi_{2j}(y,z,\omega)$:

$$\Psi_j(y,z,\omega)=\begin{pmatrix}\psi_{1j}(y,z,\omega)\\ \psi_{2j}(y,z,\omega)\end{pmatrix}. \quad (6)$$

From Eqs. (3), (4a), and (4b), we can obtain the transfer matrix relating $\Psi_j(y_{j-1}+\Delta_y,z_{j-1}+\Delta z,\omega)$ to $\Psi_{j-1}(y_{j-1},z_{j-1},\omega)$:

$$\Psi_j(y_{j-1}+\Delta y,z_{j-1}+\Delta z,\omega)=\exp[ik_y^{(j)}\Delta y]M_j(\Delta z,\omega)\times\Psi_{j-1}(y,z,\omega), \quad (7)$$

where

$$M_j(\Delta z,\omega)=\begin{pmatrix}\cos[k_z^{(j)}\Delta z] & i\frac{1}{p_j}\sin[k_z^{(j)}\Delta z]\\ ip_j\sin[k_z^{(j)}\Delta z] & \cos[k_z^{(j)}\Delta z]\end{pmatrix}, \quad (8)$$

with $p_j=[1/n_j(\omega)]\cos\theta_j$. From Eq. (4c), the z component of the electric field can be determined by

$$\psi_{3j}(y_{j-1}+\Delta y,z_{j-1}+\Delta z,\omega)=\frac{1}{n_j(\omega)}\sin\theta_j\psi_{1j}(y_{j-1}+\Delta y,z_{j-1}+\Delta z,\omega). \quad (9)$$

Therefore, we know the electromagnetic fields inside each layer. Because $\psi_{1j}(y,z,\omega)$ and $\psi_{2j}(y,z,\omega)$ are proportional to the tangential components of the magnetic and electric fields, respectively, they are continuous functions across the interface of each layer. At any position (y,z), $\Psi(y,z,\omega)$ connects with $\Psi(y_0,z_0,\omega)$ through a propagation matrix. Therefore, in the jth layer ($y_{j-1}<y<y_j$, $z_{j-1}<z<z_j$), the field at the position ($y=y_{j-1}+\Delta y$, $z=z_{j-1}+\Delta z$) is

$$\Psi(y_{j-1}+\Delta y,z_{j-1}+\Delta z,\omega)=Y(y_{j-1}+\Delta y,\omega)Q(z_{j-1}+\Delta z,\omega)\times\Psi(y_0,z_0\omega), \quad (10)$$

where

$$Y(y_{j-1}+\Delta y,\omega)=\exp[ik_y^{(j)}\Delta y]\prod_{i=1}^{j-1}\exp[ik_y^{(i)}\Delta y_i] \quad (11)$$

and

$$Q(z_{j-1}+\Delta z,\omega)=M_j(\Delta z,\omega)\prod_{i=1}^{j-1}M_i(d_i,\omega), \quad (12)$$

and d_i is the thickness of the ith layer. This equation also can be rewritten in another form $\Psi(y_{j-1}+\Delta y,z_{j-1}+\Delta z,\omega)$

$=Y(y_{j-1}+\Delta y,\omega)\Psi(y_0,z_{j-1}+\Delta z,\omega)$, where $\Psi(y_0,z_{j-1}+\Delta z,\omega)=Q(z_{j-1}+\Delta z,\omega)\Psi(y_0,z_0,\omega)$. Thus we have the matrix Q, which is only related to the transformation in the z direction, and the factor $Y(y_{j-1}+\Delta y,\omega)$, which is only related to the phase shift in the y direction. From Eqs. (9) and (10), we can calculate the electric and magnetic fields at any position provided that $\Psi(y_0,z_0,\omega)$ is known. $\Psi(y_0,z_0,\omega)$ can be determined by matching the boundary condition. As shown in Fig. 1, we assume that the light is incident from the region $z<0$ at any incident angle. In this region the field is a superposition of the incident and reflective fields, so at the incident end $(0,0)$, we have

$$\psi_1(0,0,\omega)=B_x^{(i)}(0,0,\omega)+B_x^{(r)}(0,0,\omega), \tag{13a}$$

$$\begin{aligned}\psi_2(0,0,\omega)&=c[E_y^{(i)}(0,0,\omega)-E_y^{(r)}(0,0,\omega)]\\&=p_0[B_x^{(i)}(0,0,\omega)-B_x^{(r)}(0,0,\omega)],\end{aligned} \tag{13b}$$

where the superscripts i and r denote the incident and reflective light, respectively. At the exit ($y=y_e$, $z=z_e$), there is only the transmitted field

$$\psi_1(y_e,z_e,\omega)=B_x^{(t)}(y_e,z_e,\omega)=B_x^{(t)}(0,z_e,\omega)\prod_{j=1}^{N}\exp[ik_y^{(j)}\Delta y_j], \tag{14a}$$

$$\begin{aligned}\psi_2(y_e,z_e,\omega)&=-cE_y^{(t)}(y_e,z_e,\omega)\\&=p_sB_x^{(t)}(y_e,z_e,\omega)\\&=p_sB_x^{(t)}(0,z_e,\omega)\prod_{j=1}^{N}\exp[ik_y^{(j)}\Delta y_j],\end{aligned} \tag{14b}$$

where $p_s=[1/n_s(\omega)]\cos\theta_s$ and $n_s(\omega)$ is the refractive index of the substrate. The superscript t denotes the transmitted field. Here y_e is determined by the sum over the transverse shift Δy_j of every layer in the y direction (i.e., $y_e=\Sigma_j\Delta y_j=\Sigma_j d_j\tan\theta_j$), and this corresponds to the total transverse shift of a light pulse in the y direction.

We assume that the incident field $B_x^{(i)}(0,0,\omega)$, the reflection field $B_x^{(r)}(0,0,\omega)$, and the transmitted field $B_x^{(t)}(0,0,\omega)$ have the relations

$$\begin{aligned}B_x^{(r)}(0,0,\omega)&=r(\omega)B_x^{(i)}(0,0,\omega),\\B_x^{(t)}(o,z_e,\omega)&=t(\omega)B_x^{(i)}(0,0,\omega),\end{aligned} \tag{15}$$

where $r(\omega)$ and $t(\omega)$ are, respectively, the magentic reflection and transmission coefficients of a monochromatic plane wave at frequency ω. Suppose that the matrix $X_N(\omega)$ connects the incident end of Eq. (13) and the exit end of Eq. (14) by

$$\begin{pmatrix}\psi_1(y_e,z_e,\omega)\\ \psi_2(y_e,z_e,\omega)\end{pmatrix}=\prod_{j=1}^{N}\exp[ik_y^{(j)}\Delta y_j]X_N(\omega)\begin{pmatrix}\psi_1(0,0,\omega)\\ \psi_2(0,0,\omega)\end{pmatrix}. \tag{16}$$

We find

$$X_N(\omega)=\prod_{j=1}^{N}M_j(d_j\omega)\equiv\begin{pmatrix}x_{11}(\omega) & x_{12}(\omega)\\ x_{21}(\omega) & x_{22}(\omega)\end{pmatrix}. \tag{17}$$

By substituting Eqs. (13)–(15) into Eq. (16), we obtain

$$r(\omega)=\frac{[p_0x_{22}(\omega)-p_sx_{11}(\omega)]-[p_0p_sx_{12}(\omega)-x_{21}(\omega)]}{[p_0x_{22}(\omega)+p_sx_{11}(\omega)]-[p_0p_sx_{12}(\omega)+x_{21}(\omega)]}, \tag{18a}$$

$$t(\omega)=\frac{2p_0}{[p_0x_{22}(\omega)+p_sx_{11}(\omega)]-[p_0p_sx_{12}(\omega)+x_{21}(\omega)]}, \tag{18b}$$

where we have used the property of $\det[X_N]=1$. In terms of $r(\omega)$ and $t(\omega)$, the reflectivity and transmissivity can be obtained by [22]

$$R=|r(\omega)|^2,\quad T=\frac{p_s}{p_0}|t(\omega)|^2. \tag{19}$$

Thus, we can express the electromagnetic field at the initial position ($y=0$, $z=0$) with the incident $B_x^{(i)}$ as follows:

$$\Psi(0,0,\omega)=B_x^{(i)}(0,0,\omega)\begin{pmatrix}1+r(\omega)\\ p_0[1-r(\omega)]\end{pmatrix}. \tag{20}$$

As is well known, the magnetic field is equal to the electric field in vacuum. So we also can write Eq. (20) as

$$\Psi(0,0,\omega)=\frac{1}{c}E^{(i)}(0,0,\omega)\begin{pmatrix}1+r(\omega)\\ p_0[1-r(\omega)]\end{pmatrix}, \tag{21}$$

where $E^{(i)}(0,0,\omega)$ is the initial incident electric field. Therefore, we are able to calculate the temporal-spatial behavior of the pulse. By Fourier transformation of Eq. (10), we have

$$\begin{aligned}\psi_1(y,z,t)&=\int\psi_1(y,z,\omega)e^{-i\omega t}d\omega\\&=\frac{1}{c}\int E^{(i)}(0,0,\omega)Y(y,\omega)\{[1+r(\omega)]Q_{11}(z,\omega)\\&\quad+p_0[1-r(\omega)]Q_{12}(z,\omega)\}e^{-i\omega t}d\omega,\end{aligned} \tag{22a}$$

$$\psi_2(y,z,t) = \int \psi_2(y,z,\omega)e^{-i\omega t}d\omega$$
$$= \frac{1}{c}\int E^{(i)}(0,0,\omega)Y(y,\omega)\{[1+r(\omega)]Q_{21}(z,\omega) + p_0[1-r(\omega)]Q_{22}(z,\omega)\}e^{-i\omega t}d\omega. \quad (22b)$$

Using Eq. (9), we also get the z component of the electric field in the jth layer:

$$\psi_3(y,z,t) = \frac{1}{c}\int \frac{1}{n_j(\omega)}\sin\theta_j E^i(0,0,\omega)Y(y,\omega)\{[1+r(\omega)] \times Q_{11}(z,\omega) + p_0[1-r(\omega)]Q_{12}(z,\omega)\}e^{-i\omega t}d\omega. \quad (22c)$$

Equations (22) describe the spatio temporal evolution of light passing through the 1DPC at any incident angle. The two components of the electric displacements $\vec{D}(y,z,t)$ can also be obtained through

$$D_y(y,z,t) = -\frac{1}{c}\int \epsilon(y,z,\omega)\psi_2(y,z,\omega)e^{-i\omega t}d\omega, \quad (23a)$$

$$D_z(y,z,t) = \frac{1}{c}\int \epsilon(y,z,\omega)\psi_3(y,z,\omega)e^{-i\omega t}d\omega. \quad (23b)$$

B. TE waves

In a homogeneous dielectric medium, where $\epsilon(x,y,z,\omega) = \epsilon(\omega)$ is independent of x, y, and z, we have the following equation for the electric field $\vec{E}$:

$$\nabla^2\vec{E}(x,y,z,\omega) + \frac{\omega^2}{c^2}\epsilon(\omega)\vec{E}(x,y,z,\omega) = 0. \quad (24)$$

For an incident pulse composed of TE plane waves, if we let the direction of the $\vec{E}$ field be in the x direction [i.e., $\vec{E} \equiv (E_x,0,0)$] as shown in Fig. 1, Eq. (24) can also be simplified to a scalar form

$$\frac{d^2E_x(y,z,\omega)}{dy^2} + \frac{d^2E_x(y,z,\omega)}{dz^2} + \frac{\omega^2}{c^2}\epsilon(\omega)E_x(y,z,\omega) = 0. \quad (25)$$

Comparing Eq. (25) with Eq. (2), we can obtain a similar solution by replacing the symbol B with the symbol E in the solution obtained in the previous subsection. The general solution of Eq. (25) in the jth layer can be expressed as

$$E_x^{(j)}(y,z,\omega) = \exp[ik_y^{(j)}\Delta y_j]\{E_x^{(+)}(y_{j-1},z_{j-1},\omega)\exp[ik_z^{(j)}\Delta z_j] + E_x^{(-)}(y_{j-1},z_{j-1},\omega)\exp[-ik_z^{(j)}\Delta z_j]\}. \quad (26)$$

Due to the relation $\vec{B}(y,z,\omega) = (1/i\omega)\nabla\times\vec{E}$, we obtain the components of the magnetic-induced field:

$$B_x^{(j)}(x,z,\omega) = 0, \quad (27)$$

$$B_y^{(j)}(y,z,\omega) = \frac{n_j(\omega)}{c}\cos\theta_j \exp[ik_y^{(j)}\Delta y_j] \times\{E_x^{(+)}(y_{j-1},z_{j-1},\omega)\exp[ik_z^{(j)}\Delta z_j] - E_x^{(-)}(y_{j-1},z_{j-1},\omega)\exp[-ik_z^{(j)}\Delta z_j]\}, \quad (28)$$

$$B_z^{(j)}(y,z,\omega) = -\frac{n_j(\omega)}{c}\sin\theta_j \exp[ik_y^{(j)}\Delta y_j] \times\{E_x^{(+)}(y_{j-1},z_{j-1},\omega)\exp[ik_z^{(j)}\Delta z_j] + E_x^{(-)}(y_{j-1},z_{j-1},\omega)\exp[-ik_z^{(j)}\Delta z_j]\}, \quad (29)$$

which is polarized in the y-z plane. We also define

$$\psi_{4j}(y,z,\omega) = E_x(y,z,\omega), \quad (30a)$$

$$\psi_{5j}(y,z,\omega) = cB_y(y,z,\omega), \quad (30b)$$

$$\psi_{6j}(y,z,\omega) = cB_z(y,z,\omega), \quad (30c)$$

such that the electric componet $\psi_{ij}(y,z,\omega)$ and "two magnetic components" $\psi_{2j}(y,z,\omega)$ and $\psi_{3j}(y,z,\omega)$ have the same unit. Using the previous subsection results, we exchange the symbols E and B and replace p_j with q_j [where $q_j = n_j(\omega)\cos\theta_j$]. Finally we obtain all the similar results for TE waves,

$$\psi_4(y,z,t) = \int \psi_4(y,z,\omega)e^{-i\omega t}d\omega$$
$$= \int E^{(i)}(0,0,\omega)Y(y,\omega)\{[1+r(\omega)]Q_{11}(z,\omega) + q_0[1-r(\omega)]Q_{12}(z,\omega)\}e^{-i\omega t}d\omega, \quad (31a)$$

$$\psi_5(y,z,t) = \int \psi_5(y,z,\omega)e^{-i\omega t}d\omega$$
$$= \int E^{(i)}(0,0,\omega)Y(y,\omega)\{[1+r(\omega)]Q_{21}(z,\omega) + q_0[1-r(\omega)]Q_{22}(z,\omega)\}e^{-i\omega t}d\omega, \quad (31b)$$

to calculate the temporal-spatial behavior of TE-plane-wave pulses, and we also obtain the z component of the magnetic field in the jth layer:

$$\psi_6(y,z,t) = -\int n_j(\omega)\sin\theta_j E^{(i)}(0,0,\omega)Y(y,\omega)\{[1+r(\omega)] \times Q_{11}(z,\omega) + q_0[1-r(\omega)]Q_{12}(z,\omega)\}e^{-i\omega t}d\omega. \quad (31c)$$

Here the electric reflection coefficient of a monochromatic plane wave at frequency ω is readily obtained by

$$r(\omega) = \frac{[q_0x_{22}(\omega) - q_sx_{11}(\omega)] - [q_0q_sx_{12}(\omega) - x_{21}(\omega)]}{[q_0x_{22}(\omega) + q_sx_{11}(\omega)] - [q_0q_sx_{12}(\omega) + x_{21}(\omega)]} \quad (32a)$$

and its electric transmission coefficient is given by

$$t(\omega) = \frac{2q_0}{[q_0 x_{22}(\omega) + q_s x_{11}(\omega)] - [q_0 q_s x_{12}(\omega) + x_{21}(\omega)]}, \tag{32b}$$

where $q_s = n_s(\omega)\cos\theta_s$, and $x_{ij}(\omega)$ $(i,j=1,2)$ are the elements of transfer matrix $X_N(\omega)$ between the fields of the incident and exit ends. The reflectivity and transmissivity are $R = |r(\omega)|^2$ and $T = (q_s/q_0)|t(\omega)|^2$. In this case, the electric displacement $D(y,z,t)$ can also be obtained through

$$D_y(y,z,t) = \int \epsilon(y,z,\omega)\psi_4(y,z,\omega)e^{-i\omega t}d\omega. \tag{33}$$

C. Poynting vector, energy density, and energy velocity

Now we consider how to get the Poynting vector, energy density, and energy velocity from the previous knowledge. For TM plane waves, we have

$$\vec{E}(y,z,t) = E_y(y,z,t)\vec{y} + E_z(y,z,t)\vec{z},$$

$$\vec{H}(y,z,t) = \frac{1}{\mu}B_x(y,z,t)\vec{x}. \tag{34}$$

So the Poynting vector in nonmagnetic medium ($\mu=1$) is given by

$$\begin{aligned}\vec{S}(y,z,t) &= \frac{c}{4\pi}\mathrm{Re}[\vec{E}(y,z,t)\times\vec{H}^*(y,z,t)]\\ &= \frac{c}{4\pi}\mathrm{Re}[-E_y(y,z,t)B_x^*(y,z,t)\vec{z} + E_z(y,z,t)B_x^*(y,z,t)\vec{y}]\\ &= \frac{1}{4\pi}\mathrm{Re}[\psi_2(y,z,t)\psi_1^*(y,z,t)\vec{z} + \psi_3(y,z,t)\psi_1^*(y,z,t)\vec{y}]\\ &= \frac{1}{4\pi}(s_z\vec{z} + s_y\vec{y}),\end{aligned} \tag{35}$$

where $\vec{y}$ and $\vec{z}$ are, respectively, the unit vectors of the x and y direction; $s_z = \psi_2(y,z,t)\psi_1^*(y,z,t)$ and $s_y = \psi_3(y,z,t)\psi_1^*(y,z,t)$. The absolute value of $\vec{S}(y,z,t)$ can be obtained by $|\vec{S}(y,z,t)| = (1/4\pi)\sqrt{s_z^2+s_y^2}$. We use this quantity to describe the magnitude of the Poynting vector, and the direction of the Poynting vector is determined by $\arctan(s_y/s_z)$. The energy density of the electromagnetic field in such media is given by

$$\begin{aligned}U(y,z,t) &= \frac{1}{8\pi}\{\mathrm{Re}[\vec{E}(y,z,t)\cdot\vec{D}^*(y,z,t)]\\ &\quad + \mathrm{Re}[\vec{H}(y,z,t)\cdot\vec{B}^*(y,z,t)]\}\\ &= \frac{1}{8\pi}\{\mathrm{Re}[E_y(y,z,t)D_y^*(y,z,t) + E_z(y,z,t)D_z^*(y,z,t)]\\ &\quad + \mathrm{Re}[H_x(y,z,t)B_x^*(y,z,t)]\}\\ &= \frac{1}{8\pi}\{\mathrm{Re}[-\psi_2(y,z,t)D_y^*(y,z,t)\\ &\quad + \psi_3(y,z,t)D_z^*(y,z,t)] + \mathrm{Re}[\psi_1(y,z,t)\psi_1^*(y,z,t)]\}.\end{aligned} \tag{36}$$

Therefore, from the definition of the energy velocity, we can obtain

$$V_E(y,z,t) = \frac{|\vec{S}(y,z,t)|}{U(y,z,t)}. \tag{37}$$

From this equation, we can find that the energy velocity is a time-dependent quantity. It should be pointed out that both the Poynting vector $\vec{S}(y,z,t)$ and the energy density $U(y,z,t)$ will been averaged in time (much longer than $1/\omega_0$ and much shorter than $1/\Delta\omega$, where ω_0 is the center frequency of the incident pulse and $\Delta\omega$ the spectral width of the incident pulse) in our numerical calculations. Below, we find that the energy velocity changes at different space-time points. In fact, we have pointed out recently that the energy velocity is always dependent on time t and position (y,z) and not a constant any more in dispersive media due to the interference between different frequency components of pulses [8,20]. We can also obtain the similar results for the TE-plane-wave pulses.

III. PARTIALLY COHERENT PULSES PROPAGATING IN 1DPC's

It is known that any real light field is always partially coherent. For stationary fields, the theory of coherence has been studied for a long time [22,23]. Recently, the theory of coherence of nonstationary fields has been established [24–26]. The correlation function of a pulse in space-time domain is the key quantity for discussing partially coherent pulses [27–29]. In this section, we will extend the previous results to the propagation of partially coherent light pulses in 1DPC's by using the correlation function. Because the propagation of the correlation function also satisfies the form of the wave equations [23], for the stationary medium, we can directly obtain the evolution equations of partially coherent pulses in the 1DPC from the previous results based on the following definition of the correlation functions, which can be used to describe the propagation of the partially coherent pulses [23]:

$$\Gamma_{EE}(y_1,z_1,t_1;y_2,z_2,t_2) = c^2\langle\vec{E}^*(y_1,z_1,t_1)\cdot\vec{E}(y_2,z_2,t_2)\rangle, \tag{38a}$$

$$\Gamma_{HH}(y_1,z_1,t_1;y_2,z_2,t_2) = \langle\vec{H}^*(y_1,z_1,t_1)\cdot\vec{H}(y_2,z_2,t_2)\rangle, \tag{38b}$$

$$\Gamma_{ED}(y_1,z_1,t_1;y_2,z_2,t_2) = c^2\langle\vec{E}^*(y_1,z_1,t_1)\cdot\vec{D}(y_2,z_2,t_2)\rangle, \tag{38c}$$

$$\Gamma_{HB}(y_1,z_1,t_1;y_2,z_2,t_2) = \langle\vec{H}^*(y_1,z_1,t_1)\cdot\vec{B}(y_2,z_2,t_2)\rangle, \tag{38d}$$

where the symbol $\langle\cdots\rangle$ denotes the ensemble average. $\Gamma_{EE}(y_1,z_1,t_1;y_2,z_2,t_2)$ and $\Gamma_{HH}(y_1,z_1,t_1;y_2,z_2,t_2)$ are the

correlation functions of the electric and magnetic fields, respectively. These two quantities are related to the intensties of the electric and magnetic fields by

$$I_E(y,z,t) = \Gamma_{EE}(y,z,t;y,z,t), \tag{39a}$$

$$I_H(y,z,t) = \Gamma_{HH}(y,z,t;y,z,t). \tag{39b}$$

$\Gamma_{ED}(y_1,z_1,t_1;y_2,z_2,t_2)$ and $\Gamma_{HB}(y_1,z_1,t_1;y_2,z_2,t_2)$ are, respectively, the "mixed" correlation functions between the electric fields and electric displacement and the magnetic field and magnetic-induced field, which are related to the average electric and magnetic energy densities in the medium:

$$w_e(y,z,t) = \frac{1}{8\pi}\,\mathrm{Re}[\Gamma_{ED}(y,z,t;y,z,t)], \tag{40a}$$

$$w_m(y,z,t) = \frac{1}{8\pi}\,\mathrm{Re}[\Gamma_{HB}(y,z,t;y,z,t)]. \tag{40b}$$

The total energy density of the electromagnetic field at any sapce-time point is given by

$$U(y,z,t) = w_e(y,z,t) + w_m(y,z,t). \tag{41}$$

Similar to the above steps, we can construct another "mixed" correlation vector between the electric and magnetic fields:

$$\vec{\Gamma}_{\vec{E}\times\vec{H}}(y_1,z_1,t_1;y_2,z_2,t_2) = \frac{c}{4\pi}\langle \vec{E}^*(y_1,z_1,t_1) \times \vec{H}(y_2,z_2,t_2)\rangle. \tag{42}$$

This mixed correlation vector is related to the Poynting vector by $\vec{S}(y,z,t)=\vec{\Gamma}_{\vec{E}\times\vec{H}}(y,z,t;y,z,t)$. Consequently, we can also get the energy velocity of the partially coherent light pulses through the 1DPC's, similar to Eq. (37).

Using the above definitions and equations [Eqs. (38)–(42)], for TM waves, we obtain the following quantities: The electric correlation function is given by

$$\begin{aligned}\Gamma_{EE}(y_1,z_1,t_1;y_2,z_2,t_2) &= \langle \psi_2^*(y_1,z_1,t_1)\psi_2(y_1,z_1,t_1) + \psi_3^*(y_1,z_1,t_1)\psi_3(y_1,z_1,t_1)\rangle \\ &= \frac{1}{c^2}\int\int W^{(i)}(0,0,\omega_1;0,0,\omega_2)Y^*(y_1,\omega_1)Y(y_2,\omega_2)\{[1+r^*(\omega_1)]Q_{21}^*(z_1,\omega_1) + p_0^*[1-r^*(\omega_1)]Q_{22}^*(z_1,\omega_2)\} \\ &\quad\times\{[1+r(\omega_2)]Q_{21}(z_2,\omega_2) + p_0[1-r(\omega_2)]Q_{22}(z_2,\omega_2)\}e^{i(\omega_1 t_1-\omega_2 t_2)}d\omega_1 d\omega_2 + \frac{1}{c^2}\int\int W^{(i)}(0,0,\omega_1;0,0,\omega_2) \\ &\quad\times\left[\frac{\sin\theta_j}{n_j(\omega_1)}\right]^*\frac{\sin\theta_l}{n_l(\omega_2)}Y^*(y_1,\omega_1)Y(y_2,\omega_2)\{[1+r^*(\omega_1)]Q_{11}^*(z_1,\omega_1) + p_0^*[1-r^*(\omega_1)]Q_{12}^*(z_1,\omega_1)\} \\ &\quad\times\{[1+r(\omega_2)]Q_{11}(z_2,\omega_2) + p_0[1-r(\omega)]Q_{12}(z_2,\omega_2)\}e^{i(\omega_1 t_1-\omega_2 t_2)}d\omega_1 d\omega_2,\end{aligned} \tag{43}$$

where $W^{(i)}(0,0,\omega_1;0,0,\omega_2)$ is the generalized spectral density of the initial light pulse at the incident end, and the subscripts j and l mean the space-time points (y_1,z_1,t_1) and (y_2,z_2,t_2) belonging to the different layers.

The magnetic correlation function is given by

$$\begin{aligned}\Gamma_{HH}(y_1,z_1,t_1;y_2,z_2,t_2) &= \langle \psi_1^*(y_1,z_1,t_1)\psi_1(y_1,z_1,t_1)\rangle = \frac{1}{c^2}\int W^{(i)}(0,0,\omega_1;0,0,\omega_2)Y^*(y_1,\omega_1)Y(y_2,\omega_2)\{[1+r^*(\omega_1)]Q_{11}(z_1,\omega_1) \\ &\quad + p_0[1-r^*(\omega_1)]Q_{12}^*(z_1,\omega_1)\}\{[1+r(\omega_2)]Q_{11}(z_2,\omega_2) + p_0[1-r(\omega_2)]Q_{12}(z_2,\omega_2)\}e^{i(\omega_1 t_1-\omega_2 t_2)}d\omega_1 d\omega_2,\end{aligned} \tag{44}$$

and the "mixed" correlation functions between the electric field and electric displacement and the magnetic field and magnetic-induced field are, respectively, given by

$$\Gamma_{ED}(y_1,z_1,t_1;y_2,z_2,t_2)=\frac{1}{c^2}\int\int W^{(i)}(0,0,\omega_1;0,0,\omega_2)\epsilon(y_2,z_2,\omega_2)Y^*(y_1,\omega_1)Y(y_2,\omega_2)\{[1+r^*(\omega_1)]Q_{21}^*(z_1,\omega_1)$$
$$+p_0^*[1-r^*(\omega_1)]Q_{22}^*(z_1,\omega_1)\}\{[1+r(\omega_2)]Q_{21}(z_2,\omega_2)+p_0[1-r(\omega_2)]Q_{22}(z_2,\omega_2)\}e^{i(\omega_1t_1-\omega_2t_2)}d\omega_1d\omega_2,$$
$$+\frac{1}{c^2}\int\int W^{(i)}(0,0,\omega_1;0,0,\omega_2)\epsilon(y_2,z_2,\omega_2)\left[\frac{\sin\theta_j}{n_j(\omega_1)}\right]^*\frac{\sin\theta_l}{n_l(\omega_2)}Y^*(y_1,\omega_1)Y(y_2,\omega_2)\{[1+r^*(\omega_1)]Q_{11}^*(z_1,\omega_1)$$
$$+p_0^*[1-r^*(\omega_1)]Q_{12}^*(z_1,\omega_1)\}\{[1+r(\omega_2)]Q_{11}(z_2,\omega_2)+p_0[1-r(\omega)]Q_{12}(z_2,\omega_2)\}e^{i(\omega_1t_1-\omega_2t_2)}d\omega_1d\omega_2 \quad (45)$$

and

$$\Gamma_{HB}(y_1,z_1,t_1;y_2,z_2,t_2)=\Gamma_{HH}(y_1,z_1,t_1;y_2,z_2,t_2). \quad (46)$$

Therefore, the field intensity and energy density can be obtained from Eqs. (39)–(41). The "mixed" correlation function vector is given by

$$\vec{\Gamma}_{\vec{E}\times\vec{H}}(y_1,z_1,t_1;y_2,z_2,t_2)=\frac{1}{4\pi}\langle\psi_2^*(y_1,z_1,t_1)\psi_1(y_2,z_2,t_2)\rangle\vec{z}+\langle\psi_3^*(y_1,z_1,t_1)\psi_1(y_2,z_2,t_2)\rangle\vec{y}$$
$$=\vec{z}\frac{1}{4\pi}\int\int W^{(i)}(0,0,\omega_1;0,0,\omega_2)Y^*(y_1,\omega_1)Y(y_2,\omega_2)\{[1+r^*(\omega_1)]Q_{21}^*(z_1,\omega_1)$$
$$+p_0^*[1-r^*(\omega_1)]Q_{22}^*(z_1,\omega_1)\}\{[1+r(\omega_2)]Q_{11}(z_2,\omega_2)+p_0[1-r(\omega_2)]Q_{12}(z_2,\omega_2)\}e^{i(\omega_1t_1-\omega_2t_2)}d\omega_1d\omega_2$$
$$+\vec{y}\frac{1}{4\pi}\int\int W^{(i)}(0,0,\omega_1;0,0,\omega_2)\left[\frac{1}{n_j(\omega)}\sin\theta_j\right]Y^*(y_1,\omega_1)Y(y_2,\omega_2)\{[1+r^*(\omega_1)]Q_{11}^*(z_1,\omega_1)$$
$$+p_0^*[1-r^*(\omega_1)]Q_{12}^*(z_1,\omega_1)\}\{[1+r(\omega_2)]Q_{11}(z_2,\omega_2)+p_0[1-r(\omega_2)]Q_{12}(z_2,\omega_2)\}e^{i(\omega_1t_1-\omega_2t_2)}d\omega_1d\omega_2. \quad (47)$$

For TE waves, we also can obtain the similar results from Eqs. (38)–(42) by using the results of the previous section.

IV. NUMERICAL RESULTS AND DISCUSSION

In this section, we first consider the propagation of coherent Gaussian pulses through the 1DPC's. Then, in the second subsection, we will discuss the propagation of partially coherent Gaussian pulses through the 1DPC's. The effect of coherence of light on the pulse propagation will be investigated in detail. It should be pointed out that all our calculations include all orders of dispersion and have no approximation.

A. Fully coherent Gaussian pulses

First, we suppose a fully coherent plane-wave Gaussian pulse is incident on the surface at $z=0$. The electric field of the Gaussian pulse at the incident surface is expressed as

$$E^{(i)}(0,0,t)=\exp\left(-\frac{t^2}{2\sigma_{\tau 0}^2}\right)\exp(-i\omega_0 t), \quad (48)$$

and its Fourier spectrum is

$$E^{(i)}(0,0,\omega)=\sigma_{\tau 0}\exp\left(-\frac{\sigma_{\tau 0}^2(\omega-\omega_0)^2}{2}\right), \quad (49)$$

where ω_0 is the carrier frequency of the pulse and $\sigma_{\tau 0}$ is the pulse width.

Suppose that the 1DPC is a quarter-wave stack and has a structure of $(HL)^5H$, which is the same as those used by Steinberg *et al.* [5,6]. Each layer is characterized by its constant refractive index $n_H=2.22$ or $n_L=1.41$. The optical thickness of each layer is $n_Hd_H=n_Ld_L=\lambda_{pc}/4$, where $\lambda_{pc}=692$ nm is the midgap wavelength of the 1DPC (which corresponds to the center frequency of the incident pulse).

In Fig. 2, we show the transmission as a function of frequency under different incident angles. From this figure, we can see that the band gap of the 1DPC's will move to a higher-frequency region as the incident angle increases. For

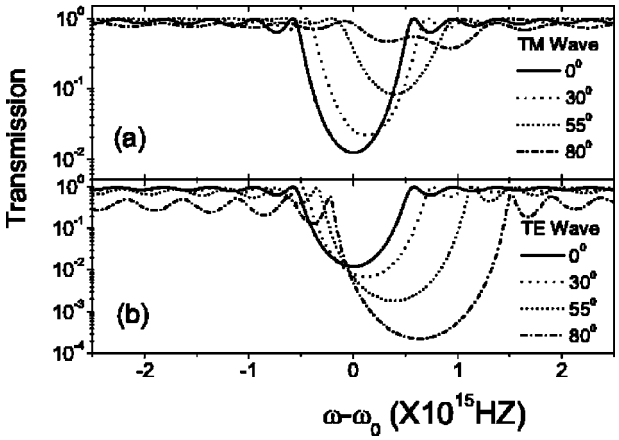

FIG. 2. Transmission of the 1DPC for (a) TM and (b) TE waves under different incident angles.

TM plane waves, as the incident angle increases, the band gap moves to a higher-frequency region and gradually disappears (the band gap closed) [30]. For TE plane waves, as the incident angle increases, although the band gap moves to a higher-frequency region, it mainly becomes larger and deeper. As is well known, the photonic band gap comes from the interference of Bragg scattering in the periodical dielectric structure. As the incident angle varies, the interference process inside the 1DPC is changed. Therefore we expect that, as the incident angle increases, the temporal behavior of light pulse in the 1DPC's will also change.

In Ref. [8], it was proved that the temporal-spatial evolutions, especially the phases of the electric and magnetic fields are different inside the 1DPC. Figure 3(a) and 3(b) show the peak time of the electric field (EF) and the magnetic field (MF) at different incident angles for the TM and TE pulses respectively. Due to the difference between EF and MF, the time delay should be defined by the peak arrival time of the energy density from Eq. (36) for the fully coherent pulses [8]. Suppose the energy density at a certain point (along the light ray trace) reaches the maximum at time t_m. The time delay can then be determined by $t_d = t_m - t_0$ ($t_0 = L_{\text{eff}}/c$ is the time delay of light passing through the vacumm, where L_{eff} is the corresponding vacuum distance between the incident end and the investigated point under any incident angle as shown in Fig. 1). The total zigzag length L_{zig} of light through the 1DPC is shown in Fig. 1. We have

$$L_{\text{zig}} = \sum_j \frac{d_j}{\cos\,\theta_j}, \tag{50}$$

and its corresponding distance L_0 of the vacuum is also shown in the figure,

$$L_{\text{eff}} = \sum_i \frac{d_i}{\cos\,\theta_i} \cos\,(\theta_0 - \theta_i), \tag{51}$$

where θ_0 and θ_i are the initial incident and refraction angles of each layer, respectively; d_i is the thickness of each layer.

Figure 3 shows the time delay t_d inside the 1DPC for the TM- and TE-plane-wave pulses under different incident angles. We find that, for both the TM- and TE-plane-wave pulses, as the incident angle increases, the time delay of the pulse increases. The reason is that the band gap of the 1DPC shifts towards a higher-frequency region.

In order to better understand the propagation of light pulses inside the 1DPC, we also use the peak time t_m (of the total energy density) to define the peak velocity by $V_M = L_{\text{eff}}(y,z)/t_m$. In Figs. 4(a) and 4(c), we show V_M as a function of the position inside the 1DPC under different incident angles. We also plot the energy velocity $V_E(z,t)$ at the time when the energy density reaches its maximum [as shown in Figs. 4(b) and 4(d)]. Comparing with the energy velocity, we find that peak velocity is completely different from the energy velocity. From Figs. 4(b) and 4(d), we can see the energy velocity never exceeds the light speed in the vacuum, while the peak velocity can exceed c. The energy velocity will be slowed by the strong interference between the incident and reflected waves inside the 1DPC (e.g., for the normal incident case). The weaker interference (for the incline incident cases), the faster energy velocity. Conversely, for the peak velocity, the strong interference between the incident and reflected waves leads to a higher peak velocity and lower energy velocity. Note that, near the exit end ($z = 1081$ nm), the energy velocity tends to be independent of the incident angle. The reason is that the interference is very weak near the exit end. We can find that, for large incident angles, the energy velocity is nearly equal to the phase velocity due to the disappearance of the PGB's, especially for the TM plane

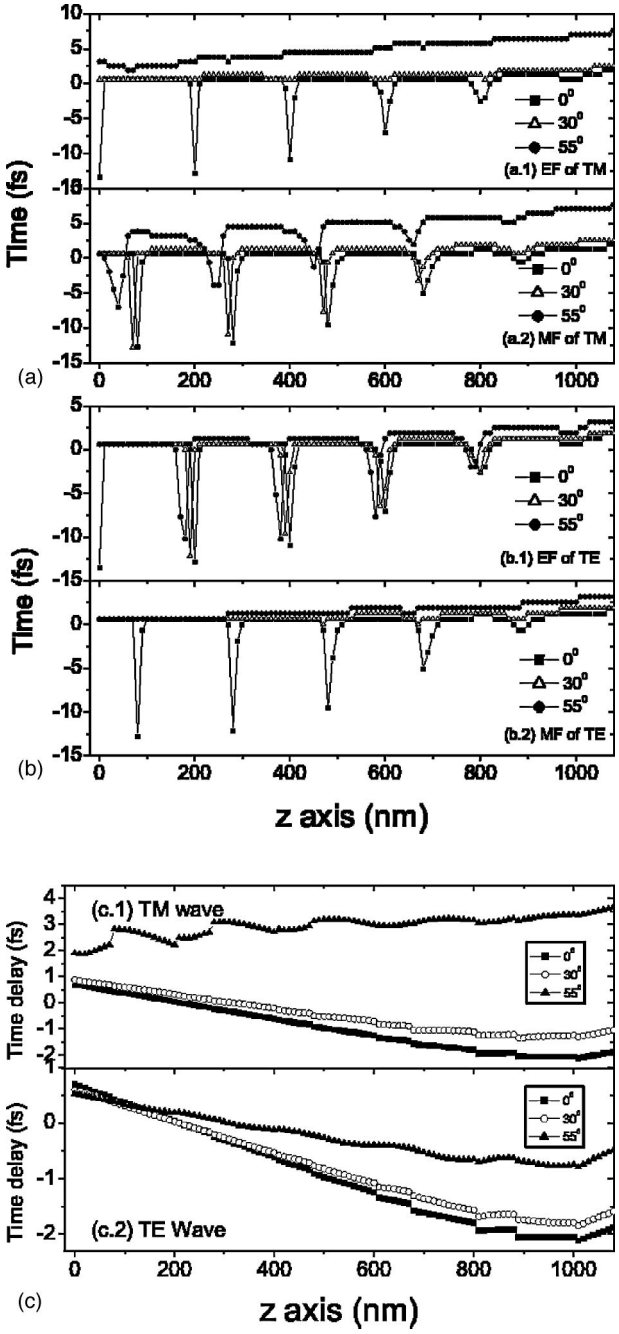

FIG. 3. Peak time of the EF and MF inside the 1DPC for (a) TM and (b) TE waves, and (c) the time delay t_d of the peak of the energy density for (c.1) TM and (c.2) TE waves under different incident angles.

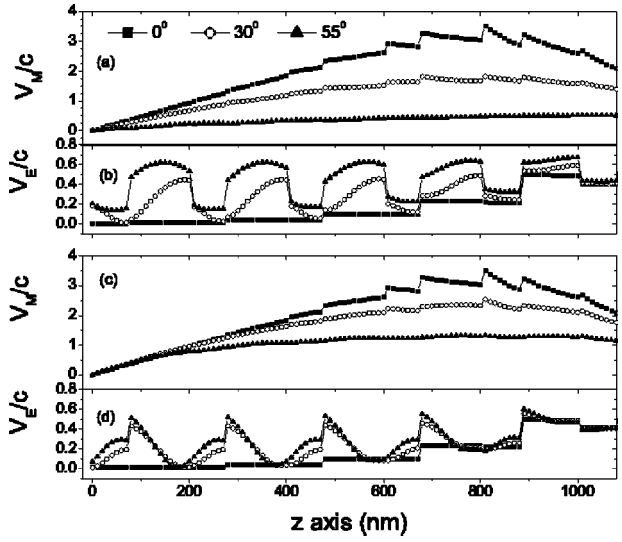

FIG. 4. Comparision between the peak velocity of the energy density and the energy velocity at the time when the energy density reaches its maximum. (a) and (b) TM waves; (c) and (d) TE waves.

wave. From these discussions, we can conclude that the evolution of the pulse passing through the 1DPC is strongly dependent on the incident angle (which will affect the strength of the Bragg scattering in the 1DPC).

B. Partially coherent Gaussian pulses

Now we turn to consider the behavior of partially coherent pulses propagating through the 1DPC. It should be pointed out that we have shown that the superluminal phenomenon is affected by the coherence of a light pulse [19]. When the coherence of a light pulse decreases, the superluminality disappears. Here we will show that how the coherence of the light pulse affects the propagation and leads to a reduction of superluminality and subluminality. It also is very important to describe the evolution of the partially coherent light pulse inside the 1DPC and its propagation properties, because, in practice, the source is always partially coherent.

First, we briefly introduce some concepts of partially coherent light pulses. For partially coherent pulses, the temporal correlation usually depends only on the time difference, and we assume that the initial correlation function is in Gaussian form:

$$\Gamma(0,0,t_1;0,0,t_2) = [I(0,0,t_1)I(0,0,t_2)]^{1/2} \times \exp\left[-\frac{(t_1-t_2)^2}{4\sigma_{L0}^2}\right]\exp[i\omega_0(t_1-t_2)], \tag{52}$$

where σ_{L0} is the correlation time width, which measures the correlation between two different space-time points. Note that the initial intensity of the light field $I(0,0,t_i) = \Gamma(0,0,t_i;0,0,t_i)$ $(i=1,2)$ is independent of σ_{L0}. That is to say, the space-time intensity profile of the pulse is the same for different values of σ_{L0}. It is obvious from Eq. (52) that a completely coherent plane-wave light pulse is obtained at the limit of $\sigma_{L0}\to\infty$; in the opposite limit of $\sigma_{L0}\to 0$, all the space-time points become uncorrelated. Therefore, when the parameter σ_{L0} varies from zero to infinity, Eq. (52) represents a class of temporal partially coherent pulses with the same space-time intensity profile, but with different coherence properties.

We can obtain the generalized cross spectral density by using the generalized Wiener-Khintchine relation [31]

$$W(0,0,\omega_1;0,0,\omega_2) = \int\int dt_1 dt_2 \Gamma(0,0,t_1;0,0,t_2)e^{i(\omega_1 t_1-\omega_2 t_2)}. \tag{53}$$

From this equation, we can obtain the generalized spectrum of partially coherent pulses.

Consider the partially coherent Gaussian pulses whose initial intensity profile is

$$I(0,0,t) = \exp\left(-\frac{t^2}{\sigma_{\tau 0}^2}\right). \tag{54}$$

The initial correlation function of the partially coherent Gaussian pulse is

$$\Gamma(0,0,t_1;0,0,t_2) = \exp\left(-\frac{t_1^2}{2\sigma_{\tau 0}^2}\right)\exp\left(-\frac{t_2^2}{2\sigma_{\tau 0}^2}\right) \times \exp\left[-\frac{(t_1-t_2)^2}{4\sigma_{L0}^2}\right]\exp[i\omega_0(t_1-t_2)]. \tag{55}$$

Substituting Eq. (55) into Eq. (53), we obtain the generalized spectral density

$$W(0,0,\omega_1;0,0,\omega_2) = \frac{1}{2\pi}\sqrt{\frac{1}{1+(\sigma_{\tau 0}/\sigma_{L0})^2}} \times \exp\left[-\frac{(\omega_1-\omega_0)^2+(\omega_2-\omega_0)^2}{2(1/\sigma_{\tau 0}^2+1/\sigma_{L0}^2)} - \frac{(\omega_1-\omega_2)^2}{4(\sigma_{\tau 0}^2+\sigma_{L0}^2)/\sigma_{\tau 0}^4}\right]. \tag{56}$$

The generalized spectral shape and width of the pulse depend on both $\sigma_{\tau 0}$ and σ_{L0}. When $\sigma_{L0}\gg\sigma_{\tau 0}$, the light pulse is essentially fully temporal correlated (fully coherent). For the partially coherent light pulses, the width of the generalized spectrum depends not only on the temporal width $\sigma_{\tau 0}$, but also on the correlated width σ_{L0}. When $\sigma_{L0}\ll\sigma_{\tau 0}$, the light pulse is globally temporal uncorrelated (incoherent), and the generalized spectral width is determined by the correlated time width σ_{L0}. Here we emphasize that the space-time profile of the pulse does not depend on σ_{L0}.

We now consider the partially coherent Gaussian pulse through the quarter-wave stack. Substituting Eq. (56) into the equations of Sec. III, we can obtain the evolution of partially

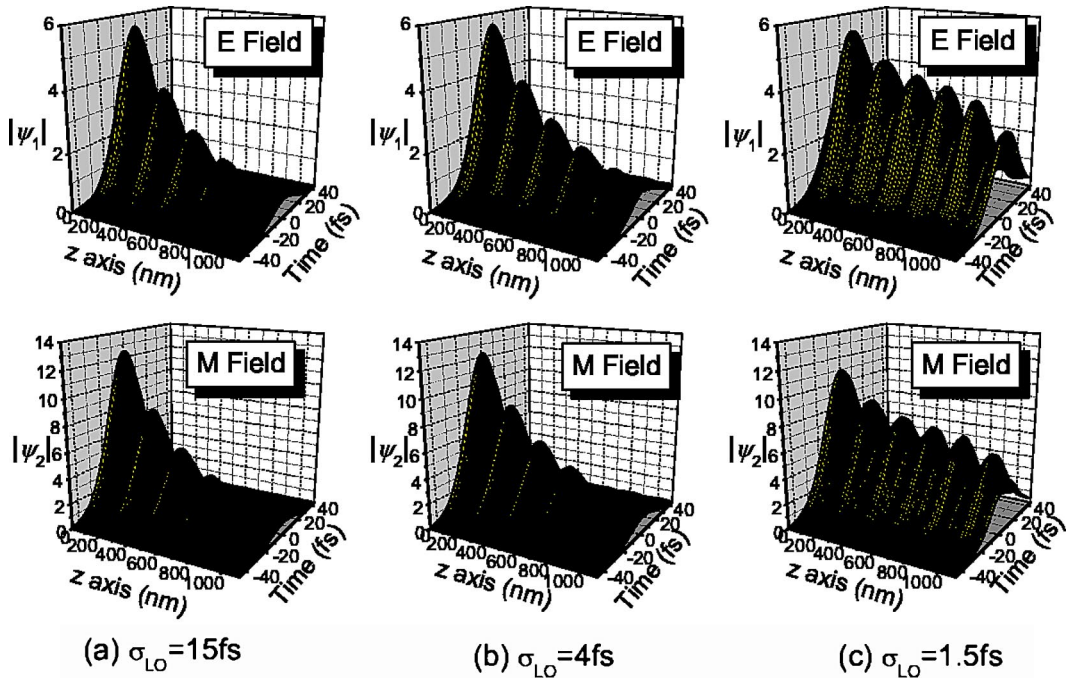

FIG. 5. Temporal-spatial evolutions of the electric and magnetic components under different correlation times (a) $\sigma_{L0}=15$ fs, (b) $\sigma_{L0}=4$ fs, and (c) $\sigma_{L0}=1.5$ fs for TM waves at normal incidence.

coherent Gaussian pulses through the 1DPC.

In Fig. 5, we show the temporal-spatial evolution for the TM plane wave at normal incidence. We find that, for the different correlation time σ_{L0}, the evolutions of the EF and MF are different. When the correlation time σ_{L0} is large (i.e., the incident field is nearly fully coherent), the evolutions of the EF and MF inside the 1DPC are similar to the case of coherent pulses [8]. From Fig. 5(a), we can find that, both EF and MF intensity profiles are strongly attenuated, and the nodes of the EF and MF are much deeper. This indicates that there exists a very strong interference between the forward and backward waves. When σ_{L0} becomes small [see Figs. 5(b) and 5(c)], the nodes of the EF and MF become unclear, and the electromagnetic fields attenuate much less than in the case of the coherent pulse. This indicates that, as the coherence decreases, the interference between the forward and backward waves becomes weaker and weaker. In Fig. 6, we show the directions of the Poynting vectors inside the 1DPC for different correlation times at normal incidence. It can be found that, as the coherence of light decreases, the interference between the forward and backward waves becomes weak, and the region of the predominated reflective wave (i.e., the reflective wave is larger than the forward wave) becomes less and less (for the lower-coherence light only in the first few layers). Thus the propagation of the pulse in the 1DPC becomes from superluminal to subluminal. This further explains how the superluminal propagation in the 1DPC is affected by the coherence of pulse.

Similar to the previous section, in Fig. 7 we plot the peak velocity V_M and the energy velocity V_E of the partially coherent pulses passing through the 1DPC with normal incidence. It can be found that the higher coherence of the light, the larger peak velocity inside the 1DPC, while for the energy velocity, it becomes larger and tends to the individual phase velocity of each layer as the coherence length of light decreases.

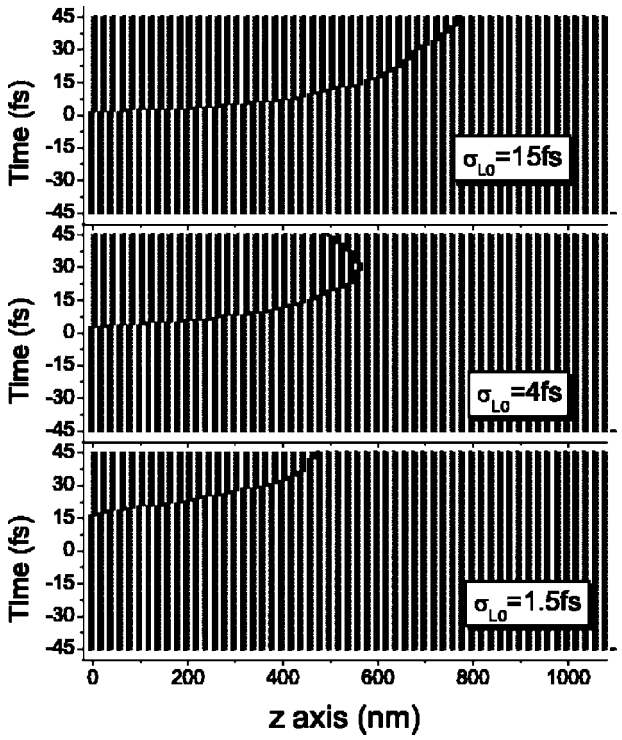

FIG. 6. Direction of the Poynting vector inside the 1DPC for TM waves at normal incidence under different correlation times.

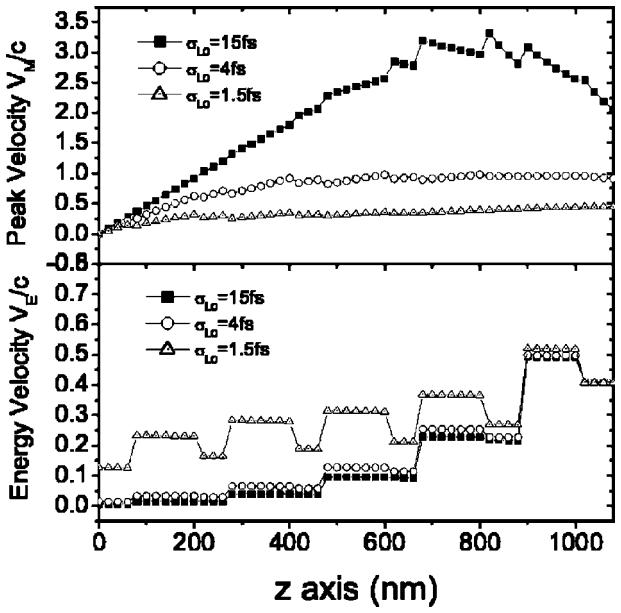

FIG. 7. Peak velocity V_M and the energy velocity V_E inside the 1DPC for TM pluses under different correlation times.

In Fig. 8, we show that the time delay as a function of the correlation time σ_{L0} at the exit end under different incident angles for two cases of TE and TM pulses. For both TM and TE plane waves, as the correlation time σ_{L0} decreases (i.e., the coherence of light decrease), the time delay increases and then gradually reaches a constant. The time delay also depends on the incident angle, and this originates from the fact that the band gap of the 1DPC will be changed. For the TM plane wave, we know that the band gap of the 1DPC will move to a higher-frequency region and gradually disappear with the increasing of the incident angle [as shown in Fig. 2(a)]. We notice that, for nearly incoherent pulses, the time delay almost tends to be the same value and is insensitive to the incident angle. For the TE plane wave, as shown in Fig. 2(b), due to the band gap becoming wide and deep and moving to the higher-frequency region, the spectrum of the pulse is gradually close to the edge of the photonic band gap. This is the reason why the time delay of coherent pulses is increased and becomes a positive. When the pulse loses its coherence, this is a similar situation in which the time delay will also tend to a constant. Figure 9 shows the shape of pulses with different correlation times σ_{L0} at the exit end under normal incidence. From this figure, it can be found that the shape of the output pulse is nearly unchanged and is similar to the one of the incident pulse when the correlation time σ_{L0} becomes very small. The time delay of the peak is different under the different correlation time σ_{L0}. Therefore, the delay time for the partially coherent light is different from that predicted by the group delay (stationary-phase approximation). The coherence of light plays a very important role for superluminal propagation media.

V. CONCLUSIONS

We have investigated the evolution of the partially coherent pulses through the one-dimensional photonic crystal

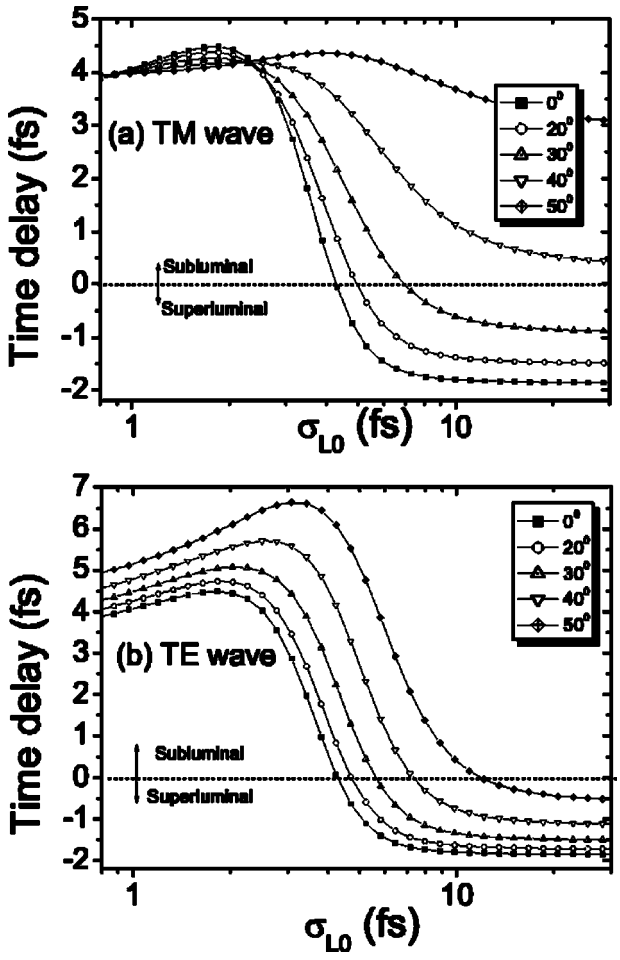

FIG. 8. Changes of the time delay as a function of the correlation time σ_{L0} under different incident angles. (a) TM waves and (b) TE waves.

(1DPC), with different incident angles. The dependence of the time delay (the delay of the peak of the energy density) on the incident angles and the coherence is discussed in detail. The velocity of the pulse peak changes from superlumi-

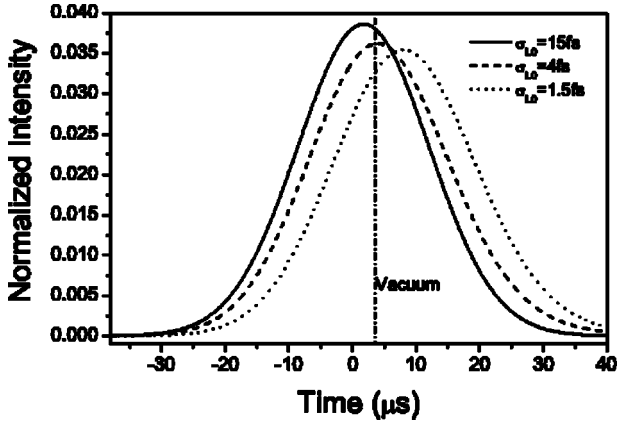

FIG. 9. Pulse profiles at the exit end for the different correlation times. The vertical dotted line denotes the peak position of pulses through the same distance vacuum.

nal to subluminal as the coherence of the pulse decreases. Changing the incident angle leads to the shift of the band gap of the 1DPC, and consequently whether the evolution of pluses inside the 1DPC is superluminal or subluminal also depends on the incident angle.

ACKNOWLEDGMENTS

This work was supported by RGC and UGC (Grant No. CA02/03.SC01) from HK Government, by the National Natural Science Foundation from China under Contract Nos. 60268001 and 60078003.

[1] E. Yablonovitch, Phys. Rev. Lett. **58**, 2059 (1987).
[2] *Photonic Band Gaps and Localization*, edited by C. M. Soukoulis (Plenum, New York, 1993).
[3] M. Büttiker and R. Landauer, Phys. Rev. Lett. **49**, 1739 (1982).
[4] A. M. Steinberg and R. Y. Chiao, Phys. Rev. A **49**, 3283 (1994).
[5] A. M. Steinberg, P. G. Kwiat, and R. Y. Chiao, Phys. Rev. Lett. **71**, 708 (1993).
[6] A. M. Steinberg and R. Y. Chiao, Phys. Rev. A **51**, 3525 (1995).
[7] Ch. Spielmann, R. Szipöcs, A. Stingl, and F. Krausz, Phys. Rev. Lett. **73**, 2308 (1994).
[8] N. H. Liu, S. Y. Zhu, H. Chen, and X. Wu, Phys. Rev. E **65**, 046607 (2002).
[9] L. Brillouin, *Propagation and Group Velocity* (Academic, New York, 1960).
[10] K. E. Oughstun and G. C. Sherman, *Electromagnetic Pulse Propagation in Causual Dielectrics* (Springer-Verlag, Berlin, 1994).
[11] J. Peatross, S. A. Glasgow, and M. Ware, Phys. Rev. Lett. **84**, 2370 (2000).
[12] S. Chu and S. Wong, Phys. Rev. Lett. **48**, 738 (1982).
[13] L. J. Wang, A. Kuzmich, and A. Dogariu, Nature (London) **406**, 277 (2000).
[14] G. Nimtz, Ann. Phys. (Leipzig) **7**, 618 (1998).
[15] R. Y. Chiao and A. M. Steinberg, *Tunneling Time and Superluminality, Progress in Optics*, Vol. 37, edited by E. Wolf (Elsevier, New York, 1997), p. 345; R. W. Boyd and D. J. Gauthier, *"Slow" and "Fast" Light, Progress in Optics*, Vol. 43, edited by E. Wolf (Elsevier, New York, 2002), p. 497.
[16] G. Nimtz and W. Heitmann, Prog. Quantum Electron. **21**, 81 (1997).
[17] D. L. Fisher and T. Tajima, Phys. Rev. Lett. **71**, 4338 (1993); P. Sprangle, J. R. Peñano, and B. Hafizi, Phys. Rev. E **64**, 026504 (2001); Chao-Guang Huang and Yuan-Zhong Zhang, Phys. Rev. A **65**, 015802 (2001); J. Opt. A, Pure Appl. Opt. **4**, 1 (2002); Filipe J. Ribeiro and Marvin L. Cohen, Phys. Rev. E **64**, 046602 (2001); Jon Marangos, Nature (London) **406**, 243 (2000); A. Dogariu, A. Kuzmich, and L. J. Wang, Phys. Rev. A **63**, 053806 (2001); A. Dogariu, A. Kuzmich, H. Cao, and L. J. Wang, Opt. Express **8**(6), 344 (2001); M. Blaauboer, A. G. Kofman, A. E. Kozhekin, G. Kurizki, D. Lenstra, and A. Lodder, Phys. Rev. A **57**, 4905 (1998); D. Bortman-Arbiv, A. D. Wilson-Gordon, and H. Friedmann, *ibid.* **63**, 043818 (2001).
[18] Y. Japha and G. Kurizki, Phys. Rev. A **53**, 586 (1996).
[19] L. G. Wang, N. H. Liu, Q. Lin, and S. Y. Zhu, Europhys. Lett. **60**, 834 (2002).
[20] L. G. Wang, N. H. Liu, Q. Lin, and S. Y. Zhu, Phys. Rev. E **68**, 066606 (2003).
[21] Jorge R. Zurita-Sánchez and P. Halevi, Phys. Rev. E **61**, 5802 (2000).
[22] M. Born and E. Wolf, *Principles of Optics*, 7th (expanded) ed. (Cambridge University Press, Cambridge, England, 1999).
[23] L. Mandel and E. Wolf, *Optical Coherence and Quantum Optics* (Cambridge University Press, New York, 1995).
[24] M. Bertolotti, A. Ferrari, and L. Sereda, J. Opt. Soc. Am. B **12**, 341 (1995).
[25] M. Bertolotti, L. Sereda, and A. Ferrari, Pure Appl. Opt. **6**, 153 (1997).
[26] L. Sereda, M. Bertolotti, and A. Ferrari, J. Opt. Soc. Am. A **15**, 695 (1998).
[27] Pertti Pääkkonen, Jari Turunen, Pasi Vahimaa, Ari T. Friberg, and Frank Wyrowski, Opt. Commun. **204**, 53 (2002).
[28] Q. Lin, L. G. Wang, and S. Y. Zhu, Opt. Commun. **219**, 65 (2003).
[29] L. G. Wang, Q. Lin, H. Chen, and S. Y. Zhu, Phys. Rev. E **67**, 056613 (2003).
[30] Y. Fink, J. N. Winn, S. Fan, C. Chen, J. Michel, J. D. Joannopoulos, and E. L. Thomas, Science **282**, 1679 (1998).
[31] J. H. Eberly and K. Wódkiewicz, J. Opt. Soc. Am. **67**, 1252 (1977).